

Document downloaded from:

<http://hdl.handle.net/10251/49098>

This paper must be cited as:

Bartovsky, P.; Domingo, LR.; Jornet Olivé, MD.; Miranda Alonso, MÁ.; Tormos Faus, RE. (2012). The triplet excited state of the biocative compound thiabendazole. Characterization and suitability as reporter for cyclodextrin complexation. *Chemical Physics Letters*. 525-526:166-170. doi:10.1016/j.cplett.2012.01.001.



The final publication is available at

<http://dx.doi.org/10.1016/j.cplett.2012.01.001>

Copyright Elsevier

The triplet excited state of the bioactive compound thiabendazole. Characterization and suitability as reporter for cyclodextrin complexation

Pavel Bartovský,¹ Luis R. Domingo,² Dolores Jornet,¹ Rosa Tormos^{1*} and Miguel A. Miranda^{1*}

¹Departamento de Química/Instituto de Tecnología Química UPV-CSIC, Universidad Politécnica de Valencia, Avenida de los Naranjos s/n, E-46022 Valencia, Spain and ²Departamento de Química Orgánica, Universidad de Valencia, Dr. Moliner 50, E 46100 Burjassot, Valencia, Spain.

mmiranda@qim.upv.es

RECEIVED DATE (to be automatically inserted after your manuscript is accepted if required according to the journal that you are submitting your paper to)

Corresponding author. Address: Instituto de Tecnología Química UPV-CSIC, Universidad Politécnica de Valencia, Avenida de los Naranjos s/n, E-46022 Valencia, Spain. Fax: +34 963877809. E-mail address: mmiranda@qim.upv.es (M. A. Miranda)

Fluorescence spectroscopy, laser flash photolysis (LFP), and density functional theory calculations have been performed to characterize the photobehavior of thiabendazole (**1**). Direct LFP of **1** results in the generation of a transient absorbing at $\lambda_{\max} = 570$ nm identified as the triplet excited state ($^3\mathbf{1}^*$). The intersystem crossing quantum yield is 0.91, and the triplet energy is 288 kJ mol^{-1} . The singlet-triplet energy gap is 84 kJ mol^{-1} .

The behavior of thiabendazole within CDs results in a marked enhanced of the triplet lifetime, this change is attributed to the mobility restrictions of included **1** imposed by the cyclodextrin cavities.

1. Introduction

Benzimidazoles (BZs) are a family of heterocyclic compounds with a broad spectrum of anthelmintic activity and are effective as anti-nematode and anti-protozoal agents.¹ In addition, many of them are used extensively on fruits and vegetables as post-harvest fungicides.² Frequently, the biological action of benzimidazoles is limited by their low solubility in water. Different strategies have been developed for enhancing the solubility of these biocides. In this context, formation of cyclodextrin inclusion complexes is frequently used by pharmaceutical industry to increase the bioavailability of poorly soluble drugs.³ As a result of complex formation the physicochemical properties of the guest molecule, such as solubility or stability, may change significantly.

In the last years, a number of members of the BZ family have attracted considerable attention due to their anti-tumoral behavior.⁴ Thus, in the course of investigations on the development of anthelmintic

resistance to BZs it has been discovered that they act binding specifically and with high affinity of the β -TUB monomer.⁵

Specifically, thiabendazole (**1**) is a bioactive benzimidazole used as human and veterinary anthelmintic.⁶ Together with its major metabolite, 5-hydroxythiabendazole, it has been monitored to trace drug residues by means of a fluorometric methodology.^{7,8} By contrast with the extensive use of **1**, the photobehavior of this compound remains relatively unknown. In fact, the studies on the photochemistry of **1** are limited to aqueous or methanolic solutions and to the effect of singlet oxygen.⁹ Thus, it has been shown that the thiazole ring is the most labile moiety of the molecule; it undergoes ring cleavage, affording benzimidazole and benzimidazole-2-carboxamide. On the other hand, the singlet excited state of **1** has been characterized, and the phosphorescence in solid matrix has also been described.¹⁰ However, the triplet excited state or other possible transients generated by photolysis of **1** in solution have not been investigated as yet. With this background, the aim of the present work is the full characterization of photophysical properties of thiabendazole triplet. This knowledge is an essential requirement to explore, in a later stage, the possibility of using the triplet excited state of **1** as a probe for host-guest interactions, such as complexation with cyclodextrin or, more interestingly, interactions with tubulin. This is connected with the recent finding that drug triplet excited states can be used as reporters for protein binding sites, as their lifetimes are markedly sensitive to the microenvironment experienced within these biomacromolecules.^{11,12,13,14}

1. Results and Discussion

In a preliminary stage, the absorption spectrum of **1** in acetonitrile was recorded. It presents a band centered at 300 nm ($\epsilon = 15000 \text{ M}^{-1}\text{cm}^{-1}$) with a shoulder at 310 nm. In aqueous solutions the shape and position of the bands are very similar to those obtained in organic solvent.

The emission spectrum of **1** in acetonitrile when excited at 281 nm accompanied by the excitation band for the emission at 350 nm, which is similar to the long-wavelength absorption band. The spectra registered in PBS/MeCN matched with those obtained in acetonitrile. From the intersection between the excitation and emission after normalization, a singlet energy of 372 kJ mol^{-1} was determined. The emission quantum yield in deaerated MeCN solution was 0.06 and in PBS/MeCN (3/1, v/v) it was found to be 0.07. These values are somewhat higher than those previously reported in MeOH.¹⁰ The fluorescence properties were insensitive to oxygen.

The phosphorescence spectrum of **1** in methanol at 77 K consisted of an almost structure less emission with a maximum at 475 nm. The triplet energy was determined as 282 kJ mol^{-1} .

1.1 Transient absorption spectroscopy

After examining the absorption and emission behavior, transient absorption spectroscopy studies were undertaken. Thus, 266 nm laser flash photolysis (LPF) of **1** in deaerated acetonitrile or PBS/MeCN (3/1, v/v) solutions led to transients absorbing in the 350-700 nm range. The spectra obtained after the laser pulse showed a broad band centered at 570 nm, which was ascribed to the T-T absorption (Figure 1). The

lifetime was found to be 1.0 μs in acetonitrile and 3.4 μs in PBS and was dependent on the concentration of **1**, with a self-quenching rate constant in the order of $10^9 \text{ M}^{-1} \text{ s}^{-1}$.

As expected for a triplet, it was sensitive to the presence of oxygen. From the Stern-Volmer plot (Figure 1, inset), a k_q value of $6.6 \times 10^9 \text{ M}^{-1} \text{ s}^{-1}$ was determined for **1** in acetonitrile.

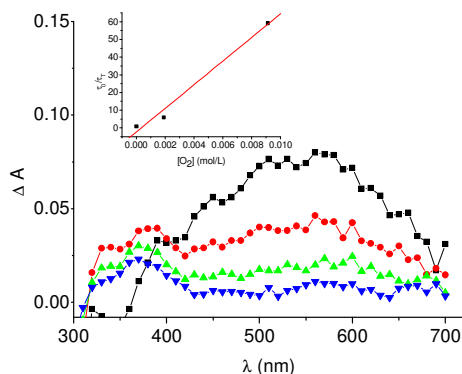


Fig. 1. Transient absorption spectra of thiabendazole ($4.0 \times 10^{-3} \text{ M}$) in MeCN after 266 nm irradiation, registered at 0.23 μs (■), 1.0 μs (●), 2.17 μs (▲) and 4.52 μs (▼) delay times. Inset: Stern-Volmer plot obtained for triplet quenching by O_2 in MeCN.

Moreover, alternative generation of the triplet by sensitization with xanthone ($E_T = 310 \text{ kJ mol}^{-1}$)¹⁵ and 4,4'-dimethoxybenzophenone ($E_T = 282 \text{ kJ mol}^{-1}$)¹⁶ was used for characterizing the transient. Thus, LFP of a deaerated xanthone solution in PBS/MeCN at 355 nm produced xanthone triplet with maximum at *ca.* 600 nm. In the presence of thiabendazole, transformation of this sharp band into a broader signal with maximum at 575 nm was observed (not shown). Figure 1 shows the growth and decay of the triplet thiabendazole signal at 500 nm, upon addition of increasing amounts of **1** to xanthone (from 0:1 to 20:1 molar ratio). From the corresponding decays at 600 nm, the rate constant of this energy transfer process was found to be $1.5 \times 10^9 \text{ M}^{-1} \text{ s}^{-1}$.

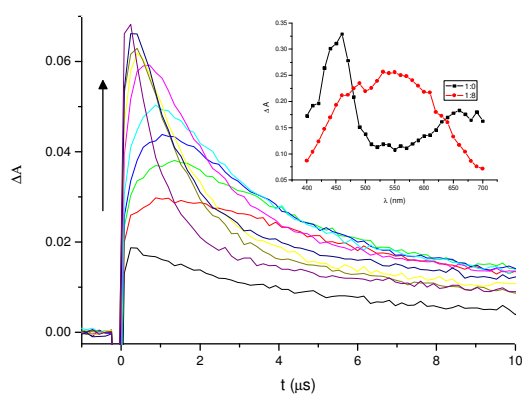


Fig. 2. Sensitization of thiabendazole triplet via energy transfer from xanthone triplet excited state in deaerated PBS/MeCN

(3:1 v/v), registration wavelength: $\lambda_{\text{reg}} = 500 \text{ nm}$. The **1**: xanthone ratios were changed from 0:1 to 20:1

Inset: Sensitization of **1** triplet via T-T energy transfer from DMBP. Excitation wavelength: $\lambda = 355 \text{ nm}$, solvent: PBS/MeCN (3:1).

Spectra of DMBP alone (■) and in the presence of **1** (●) recorded 0.4 μs after the laser pulse

Likewise, when the sensitizer was 4,4'-dimethoxybenzophenone (DMBP) deactivation of the aromatic ketone triplet occurred with the concomitant appearance of the **1** triplet. This is clearly shown in Figure 2 (inset).

In this case, the rate constant for energy transfer was $3.9 \times 10^8 \text{ M}^{-1} \text{ s}^{-1}$, one order of magnitude lower than that obtained for xanthone, indicating that the triplet energies of **1** and DMBP must be close to each other.

In addition, different triplet acceptors *trans*-stilbene, acenaphthene and naphthalene were used to quench the T-T absorption band of **1**; the rate constants for the involved processes were $1.0 \times 10^9 \text{ M}^{-1} \text{ s}^{-1}$, $9.8 \times 10^9 \text{ M}^{-1} \text{ s}^{-1}$ and $5.5 \times 10^9 \text{ M}^{-1} \text{ s}^{-1}$, respectively

Overall, the above data indicate that the triplet energy of thiabendazole must be close to 282 kJ mol^{-1} . In order to obtain a narrower range for this parameter, quenching of the T-T absorption of DMBP in PBS:acetonitrile was investigated by LFP at 355 nm, in the presence of increasing amounts of several acceptors¹⁵ including **1**. The decay of the 430 nm band was analyzed, to determine the quenching rate constants. When the reciprocal DMBP triplet lifetimes were plotted against the quencher concentrations, different straight lines were obtained (not shown); their slopes (intermolecular k_{ET} values) are given in Table 1.

Table 1.

Rate Constants for Energy Transfer from DMBP to Quenchers

	E_{T} kJ mol ⁻¹	$k_{\text{ET}}(\text{M}^{-1} \text{ s}^{-1})$ PBS:MeCN
1,3-cyclohexadiene	219	4.02×10^9
biphenyl	271	4.90×10^9
fluorene	282	4.60×10^9
dibenzofuran	289	2.80×10^8
thiabendazole	$E_{\text{T}}(\mathbf{1})$	3.90×10^8

The rate constant of triplet-triplet energy transfer (k_{ET}) depends on the triplet energy gap (ΔE_{T}), between the donor and the acceptor, as given by Sandros' equation¹⁷ (1)

$$k_{\text{ET}} = (k_{\text{max}} \times e^{-\Delta E_{\text{T}}/RT}) / (e^{-\Delta E_{\text{T}}/RT} + 1) \quad (1)$$

where k_{max} is the optimum rate constant for the system. Thus, assuming a value of $k_{\text{max}} = 4.5 \times 10^9 \text{ M}^{-1} \text{ s}^{-1}$, chosen as the average of the first three entries, ΔE_{T} resulted to be 6 kJ mol^{-1} . Therefore, the triplet energy value of **1** is $E_{\text{T}}(\mathbf{1}) 288 \text{ kJ mol}^{-1}$.

Furthermore, the molar absorption coefficient of thiabendazole triplet was determined using DMBP as standard ($\epsilon = 2700 \text{ mol L}^{-1} \text{ cm}^{-1}$ at 450 nm). In PBS/MeCN (3/1, v/v); it was found to be $3960 \text{ mol L}^{-1} \text{ cm}^{-1}$. The intersystem crossing (ISC) quantum yield (Φ_{ISC}) of **1** in PBS/MeCN was calculated from the ΔOD of the T-T bands for isoabsorptive solutions of **1** and DMBP, taking into account the molar absorption coefficients of the two triplets and the known ISC quantum yield of DMBP (0.97). Its value was established at ca. 0.91.

1.2 Theoretical DFT calculations

Geometry optimization. The ground state geometry of **1** was first analyzed. Due to the free bond rotation around the C1-C6 single bond (see numbering scheme in Figure 3), two rotamers (**1-c** and **1-t**) are feasible, where the NH group of benzimidazole and the N atom of thiazole present a *s-cis* or a *s-trans* arrangement. Hence, a conformational analysis was performed in order to characterize the most favorable structure.

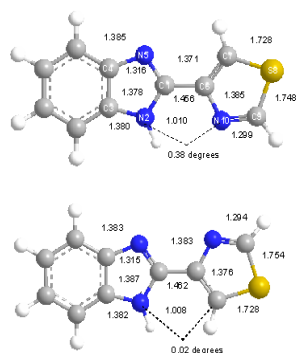


Fig. 3. B3LYP/6-31G(d) **1-c** (top) and **1-t** (bottom) structures. The lengths are given in Angstroms.

According to B3LYP/6-31G(d) optimization, **1-t** is 31.7 kJ mol⁻¹ higher in energy than **1-c**. The interconversion between both conformers occurs via structure **1-90**, in which the two heterocyclic systems are twisted 90 degrees, with an activation energy of 47 kJ mol⁻¹. Although this cannot be considered a high barrier, based on the energy difference between **1-c** and **1-t** only the former will be considered in the singlet excitation study. Similar relative energies were obtained by full optimization at the B3LYP/6-311+G(d,p) level (see Table 2). A comparison between the B3LYP/6-31G(d) and B3LYP/6-311+G(d,p) geometries did not reveal significant differences, either.

Table 2

	Total (E in a.u.) and Relative Energies (ΔE in kJ mol ⁻¹) of the 1-c , 1-90 and 1-t Structures			
	B3LYP/6-31G(d)		B3LYP/6-311+G(d,p)	
	E	ΔE	E	ΔE
1-c	-947.7350696		-947.902007	
1-90	-947.7194715	41	-947.887831	37
1-t	-947.7230448	32	-947.889882	32

Some geometrical parameters, together with the Wiberg bond order (BO) deserve special comments; they include: i) the C1-C6 bond length, 1.456 Å, and the corresponding BO value, 1.06, which point to a Csp²-Csp² single bond, ii) the two S-C bond lengths, 1.728 and 1.748 Å, and the BO value, 1.21, characteristic of S-C single bonds with a slight π character; iii) the C6-C7 and the C9-N10 bond lengths, 1.371 and 1.299 Å, and the BO value, 1.56 and 1.65, suggesting a marked π character, and iv) the N2-C1-C6-N10 dihedral angle, 0.38 degrees, which accounts for the planar arrangement. The C1-C6 BO value indicates lack of conjugation between both ring systems in clear agreement with the low energy barrier associated with rotation around the C1-C6 bond.

Singlet and triplet excitation. The first three singlet and triplet excited states of **1-c** were studied at the time-dependent (TD) B3LYP/6-311+G(d,p) level using the B3LYP/6-311+G(d,p) geometry. The excitation energies and oscillator strengths are given in Table 3.

Table 3.

TD B3LYP/6-311+G(d,p) Excitation Energies (EE in nm), Oscillator Strengths (f) and Relative Energies ^{a,b} (ΔE in kJ mol⁻¹) of the First Three Singlet and Triplet Excited States of **1-c**.

Excited State	Transition	EE	f	ΔE
S1	52 $\pi \rightarrow$ 53 π^* (0.6490)	307.1	2462	389 (398)

S2	51 $\pi \rightarrow 53 \pi^*$ (0.6760)	291.7	0573	410 (423)
S3	52 $\pi \rightarrow 54 \pi^*$ (0.6399)	270.1	3354	443 (450)
T1	52 $\pi \rightarrow 53 \pi^*$ (0.7026)	434.8	0000	275 (284)
T2	51 $\pi \rightarrow 53 \pi^*$ (0.5016)	364.6	0000	328 (333)
T3	52 $\pi \rightarrow 54 \pi^*$ (0.5360)	326.4	0000	366 (372)

^{a)} The TD B3LYP/6-311+G(d,p) total energy of S0 ground state of **1-c** is -947.902007 (gas phase) and -947.921668 (acetonitrile) a.u.

^{b)} In parenthesis relative energies in acetonitrile.

In order to characterize the main molecular orbital (MO) contributors to these singlet and triplet excitations, B3LYP/6-31G(d) MOs 51 to 54 were analyzed. While MOs 51 and 52 correspond to HOMO-1 and HOMO, MOs 53 and 54 correspond to LUMO and LUMO+1, respectively. The four MOs show a π symmetry.

The first S1 singlet excited state presents an excitation energy of 307.1 nm ($f = 0.2462$) and corresponds mainly to a $\pi \rightarrow \pi^*$ excitation between HOMO and LUMO. It is located 389 kJ mol⁻¹ above the S0 ground state.

The S2 singlet excited state presents an excitation energy of 291.7 nm ($f = 0.0573$), corresponding to a $\pi \rightarrow \pi^*$ excitation between HOMO-1 and LUMO, and is located 410 kJ mol⁻¹ above the S0 ground state. Finally, the S3 singlet excited state presents an excitation energy of 270.1 nm ($f = 0.3354$) and is basically associated with a $\pi \rightarrow \pi^*$ excitation between HOMO-1 and LUMO+1. It is located 443 kJ mol⁻¹ above the S0 ground state.

The first T1 triplet state, generated by a $\pi \rightarrow \pi^*$ excitation between HOMO and LUMO presents an excitation energy of 434.8 nm and is located 275 kJ mol⁻¹ above the S0 ground state. The T2 triplet excited state (excitation energy of 364.6 nm) is associated with a $\pi \rightarrow \pi^*$ excitation between HOMO-1 and LUMO and is located 328 kJ mol⁻¹ above the S0 ground state. The T3 triplet excited state, with excitation energy of 326.4 nm, results from a $\pi \rightarrow \pi^*$ excitation between HOMO-1 and LUMO+1 and is located 366 kJ mol⁻¹ above the S0 ground state.

Finally, the solvent effects (acetonitrile) on the energies of these singlet and triplet excited states were studied using the polarizable continuum model (PCM) by TD B3LYP(PCM)/6-311+G(d,p) calculations over the gas phase geometries. The relative energies are given in Table 4. For the singlet states the relative energies are 398 (S1), 423 (S2) and 450 (S3) kJ mol⁻¹, while the triplet states are 284 (T1), 333 (T2) and 372 (T) kJ mol⁻¹. Therefore, inclusion of solvent effects through a continuum model increases slightly the gas phase energies between 4-9 kJ mol⁻¹.

2.3 Formation of cyclodextrin inclusion complexes

In order to study the influence of microheterogeneous media on the behavior of the triplet excited state, **1** was included within α , β and γ cyclodextrins (CDs). The formation stoichiometry and topology of complexes has been previously investigated by means of different techniques, such as ¹HNMR, IR, fluorescence, solubility and absorption spectrophotometry. Thus, formation of the 1:1 complexes with moderate association constants has been determined for the three types of CDs.³

When solutions of **1** (4×10^{-5} M) and CD in neutral buffer (0.05 M PBS) were submitted to LFP the transient absorption spectra obtained after laser excitation ($\lambda_{\text{exc}} = 266$ nm) were similar (Figure 4, upper inset) to that obtained for **1** in acetonitrile, although the signal intensity was higher than in the bulk solution. Figure 4A shows a clear increase of the triplet absorption signal with the $[\beta\text{-CD}]/\mathbf{1}$ molar ratio; however, for solubility limitations it was not possible to reach a plateau. The association constant (K_A) value was determined from the relationship between the changes observed in the absorption (ΔA) at 570 nm as a function of the total cyclodextrin concentration $[\text{CD}]_T$ (Figure 4). It can be related to the equilibrium complex formation according to Benesi-Hildebrand (eq 1) expression¹⁸ where $\Delta\varepsilon$ is the difference between the molar absorption coefficients for complexed and free thiabendazole.

$$1/\Delta A = 1/\Delta\varepsilon[\mathbf{1}]_T + 1/K_A \Delta\varepsilon [\mathbf{1}]_T [\text{CD}]_T \quad (1)$$

From the values of intercept and slope of the straight lines fitted to the experimental data the association constant was estimated as 135 M^{-1} , which is in reasonable agreement with the values obtained for the same system by means of fluorescence or solubility measurements (ca. 100 M^{-1}).³ To our knowledge this is the first example where laser flash photolysis has been used to obtain the association constant for a CD complex.

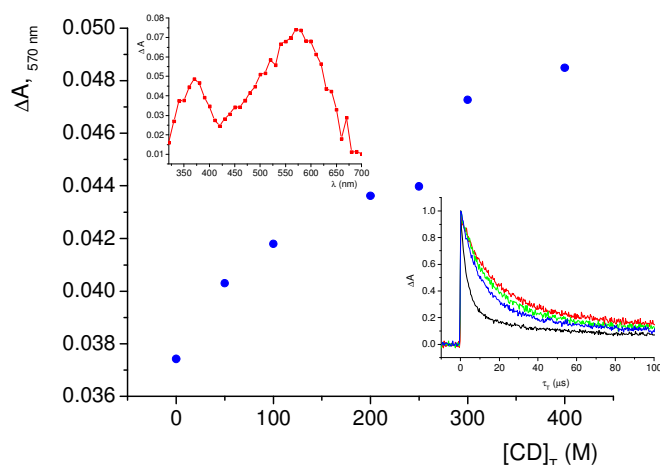


Fig. 4. Dependence of thiabendazole transient absorption signal at $\lambda_{\text{max}} = 570$ nm versus β -CD molar concentration in aqueous solutions, at 25 °C. Upper inset: transient absorption spectrum obtained by 266 nm laser flash photolysis of **1** (4×10^{-5} M) in the presence of β -CD (1:440) registered 0.31 μs after the pulse. Lower inset: Normalized decays monitored at 570 nm for **1** (4×10^{-5} M) in PBS, and in the presence of α -CD (1:400) ●, β -CD (1:440) ● and γ -CD (1:600) ●

The decays monitored at 570 nm in air equilibrated solutions, in the absence of CDs, fitted well with a first order kinetics. Conversely, in the presence of CDs two lifetimes, corresponding to the free and complexed forms, were necessary to fit the decays. As shown in Figure 4 lower inset, in the microheterogeneous system decays were markedly longer than in solution (3.4 μs , 12.2 μs , 14.2 μs , 9.5 μs bulk solution, α , β and γ CD, respectively).

This observation can be attributed to a slow-down of non radiative decay processes associated with the limited degrees of freedom.

The longest lifetime was displayed by the **1**@ β -CD complex, and the shortest by **1**@ γ -CD complex. This must be related to the relative size of the CD cavities, which determines the degree of interaction. Interestingly, the triplet behavior was parallel to that shown by the singlet excited state in the same microenvironment. In fact when the fluorescence or triplet absorption signals I/I_0 (at 350 and 570, respectively) were plotted *versus* the $[\beta\text{-CD}]/[\mathbf{1}]$ ratio, nearly superimposable trends were observed (Figure 5). Thus, a clear correlation exists between the singlet and triplet properties, as regards complexation with CD.

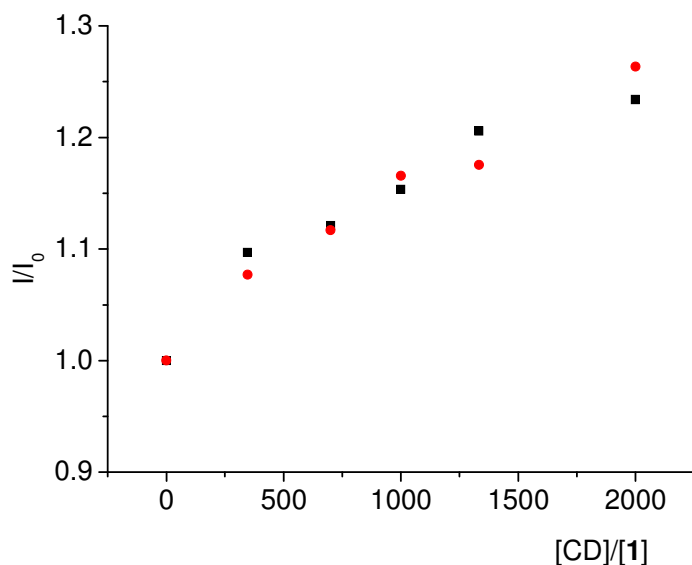


Fig. 5. Dependence of I/I_0 on β -CD/**1** ratio by laser flash photolysis (●) and fluorescence measurements (■).

3. Conclusions

Laser flash photolysis of thiabendazole at 266 nm gives rise to its $\pi\pi^*$ triplet excited state, detected as a broad transient absorption with maximum at 570 nm. The intersystem quantum yield is very high (0.91) and the triplet energy is 288 kJ mol^{-1} .

The triplet lifetime is markedly medium dependent, increasing from $3.4 \mu\text{s}$ in aqueous solution to $14.2 \mu\text{s}$ within the β -CD cavities. The intensity of the T-T signal also increases upon CD complexation; this change has been used to determine the binding constant, which has been estimated as 134 M^{-1} for β -CD. This result is in good agreement with the value obtained by means of fluorescence measurements.

4. Experimental section

4.1. Materials and Solvents

Thiabendazole (**1**), xanthone, 4,4'-dimethoxybenzophenone, 1,3-cyclohexadiene, *trans*-stilbene, acenaphthene, naphthalene, biphenyl, fluorene and dibenzofuran were purchased from Aldrich. Their purity was checked by $^1\text{H-NMR}$ spectroscopy and high performance liquid chromatography (HPLC) analysis. Reagent grade solvent acetonitrile was purchased from Scharlau and used without further purification.

4.2. Absorption Spectra

Optical spectra in different solvents were measured on a Perkin Elmer Lambda 35 UV/Vis spectrophotometer. Emission spectra were recorded on a spectrofluorometer system, which was provided with an M 300 emission monochromator in the wavelength range of 200–900 nm and are uncorrected. Samples were placed into 10 × 10 mm² Suprasil quartz cells with a septum cap. Solutions were purged with nitrogen or oxygen for at least 10 min before the measurements. Fluorescence quantum yields were determined using *S*-flurbiprofen [*S*-2-fluoro- α -methyl-4-biphenylacetic acid] as reference ($\Phi_F = 0.27$ at $\lambda_{exc} = 281$ nm in methanol as solvent).⁽¹⁷⁾ The absorbance of the samples at the excitation wavelength was kept below 0.1. Excitation and emission slits were maintained unchanged during the emission experiments. For time-resolved fluorescence decay measurements, the conventional single photon counting was used. All experiments were performed at room temperature (22 °C).

4.3. Laser Flash Photolysis (LFP)

The LFP experiments were carried out by using a Q-switched Nd:YAG laser (Quantel Brilliant, 266 or 355 nm, 10 or 14 mJ per pulse, 5 ns fwhm) coupled to a mLFP-111 Luzchem miniaturized equipment. This transient absorption spectrometer includes a ceramic xenon light source, 125 mm monochromator, Tektronix 9-bit digitizer TDS-3000 series with 300 MHz bandwidth, compact photomultiplier and power supply, cell holder and fiber optic connectors, fiber optic sensor for laser-sensing pretrigger signal, computer interfaces and a software package developed in the LabVIEW environment from National Instruments. The LFP equipment supplies 5 V trigger pulses with programmable frequency and delay. The risetime of the detector/digitizer is approximately 3 ns up to 300 MHz (2.5 GHz sampling). The laser pulse is probed by a fiber that synchronizes the LFP system with the digitizer operating in the pretrigger mode. All transient spectra were recorded using 10 × 10 mm² quartz cells with 4 mL capacity, and all were bubbled during 20 min with N₂. Absorbance of the samples was kept between 0.2 and 0.3 at the laser wavelength. All the experiments were carried out at room temperature.

4.4. Computational Methods

Density functional theory (DFT) calculations were carried out using the B3LYP¹⁹ exchange correlation functional, together with the 6-31G(d) and 6-311+G(d,p) basis sets.²⁰ Optimizations were carried out using the Berny analytical gradient optimization method.^{21,22} Electronic structures of stationary points were analyzed using the Wiberg indices.^{23,24} Vertical energies of the singlet and triplet excited states were calculated using the time-dependent (TD-DFT) method.^{25,26} Solvent effects of acetonitrile on the excited states were considered by TD-DFT calculation on the gas-phase structures using a self-consistent reaction field (SCRFF)²⁷ based on the polarizable continuum model (PCM) of the Tomasi's group.^{28,29} All calculations were carried out with the Gaussian 03 suite of programs.³⁰

Acknowledgment. Financial support from the MICINN (Grants: CTQ2009-11027/BQU, CTQ2010-19909 and pre-doctoral fellowship to P.B.) and the Generalitat Valenciana (Prometeo Program) is gratefully acknowledged.

References and notes

- [1] R.K. Prichard, *Parasitology* 134 (2007) 1087
- [2] H. Das, S. Jayaraman, M. Naika, A. S. Bawa, *J. Food Sci. Technol.* 44 (2007) 237.
- [3] M. Lezcano, W. Al-Soufi, M. Novo, E. Rodriguez-Núñez, J. Vázquez Tato, *J. Agric. Food Chem.* 50 (2002) 108.
- [4] M. E. Steams, M. Wang, K. Fudge, *Cancer Res.* 53 (1993) 3073
- [5] G. W. Lubega, T.G. Geary, R. D. Klein, R. K. Prichard, *Mol. Biochem. Parasitol.* 62 (1993), 281.
- [6] L. Srikanth, V. Varun Raj, N. Raghunandan, L. Venkateshwerlu, *Pharma Chemica* 3 (2011) 172
- [7] Watts, M. T.; Raisys, V. A.; Bauer, L. A. *J. Chromatog.* 230 (1982) 79
- [8] G. E. Hardee, M. A. Tshabalala, J. N. Moore, R. D. Gokhales, *Res. Vet. Sci.* 43 (1987) 13.
- [9] M.R. Mahran, M.M. Sidky, H Wamhoff, *Chemosphere* 12 (1983) 1611.
- [10] P.C Tway, L.J. Cline Love, *J. Phys. Chem.* 86 (1982) 5223.
- [11] M C. Jiménez, M. A. Miranda, I. Vayá, *J. Am Chem. Soc.* 127 (2005) 10134.
- [12] V. Lhiaubet-Vallet, Z. Sarabia, F. Bosca, M. A. Miranda, *J. Am. Chem. Soc.* 126 (2004) 9538
- [13] V. Lhiaubet-Vallet, F. Bosca, M. A. Miranda, *J. Phys. Chem. B.* 111 (2007) 423
- [14] I. Vayá, C. J. Bueno, M. C. Jiménez, M. A. Miranda, *Chem. Eur. J.* 14 (2008) 11284.
- [15] S.L. Murov, I. Carmichael, G.L. Hug, *Handbook of Photochemistry*, Marcel Dekker, Inc.; New York, 2nd edn., 1993.
- [16] D. Jornet, R. Tormos, M. A. Miranda, *J. Phys. Chem. B.* 115 (2011) 10768.
- [17] K. Sandros, *Acta Chem. Scand.* (1964) 2355.
- [18] H.A. Benesi, J.H. Hildebrand, *J. Am. Chem. Soc.* 71 (1949) 2703.
- [19] C. Lee, W. Yang, R. G. Parr, *Phys. Rev. B* 37 (1998) 785
- [20] W. J. Hehre, L. Radom, P. v. R. Schleyer, J. A. Pople, *Ab initio Molecular Orbital Theory*; Wiley: New York, 1986.
- [21] H. B. Schlegel, *J. Comput. Chem.* 3 (1982) 214

- [22] Schlegel, H. B. Geometry Optimization on Potential Energy Surface. In *Modern Electronic Structure Theory*; Yarkony, D. R., Ed.; World Scientific Publishing: Singapore, 1994.
- [23] K. B. Wiberg, *Tetrahedron* 24 (1968) 1083.
- [24] A. E. Reed, R. B. Weinstock, F. J. Weinhold, *Chem. Phys.* 83 (1985) 735.
- [25] R. Bauernschmitt; Ahlrichs, R. *Chem. Phys. Lett.* 256 (1996) 454
- [26] M. E. Casida, C. Jamorski, K. C. Casida, D. R. Salahud, *J. Chem. Phys.* 108 (1998) 4439.
- [27] J. Tomasi, M. Persico, *Chem. Rev.* 94 (1994) 2027
- [28] E. Cancès, B. Mennucci, J. Tomasi, *J. Chem. Phys.* 107 (1997) 3032
- [29] Barone, V., Cossi, M., Tomasi, J. *J. Comput. Chem.* 19 (1998) 404.
- [30] M. J. Frisch, G. W. Trucks, H. B. Schlegel, G. E. Scuseria, M. A. Robb, J. R. Cheeseman, J. A. Jr. Montgomery, T. Vreven, K. N. Kudin, J. C. Burant, J. M. Millam, S. S. Iyengar, J. Tomasi, V. Barone, B. Mennucci, M. Cossi, G. Scalmani, N. Rega, G. A. Petersson, H. Nakatsuji, M. Hada, M. Ehara, K. Toyota, R. Fukuda, J. Hasegawa, M. Ishida, T. Nakajima, Y. Honda, O. Kitao, H. Nakai, M. Klene, X. Li, J. E. Knox, H. P. Hratchian, J. B. Cross, C. Adamo, J. Jaramillo, R. Gomperts, R. E. Stratmann, O. Yazyev, A. J. Austin, R. Cammi, C. Pomelli, J. W. Ochterski, P. Y. Ayala, K. Morokuma, G. A. Voth, P. Salvador, J. J. Dannenberg, V. G. Zakrzewski, S. Dapprich, A. D. Daniels, M. C. Strain, O. Farkas, D. K. Malick, A. D. Rabuck, K. Raghavachari, J. B. Foresman, J. V. Ortiz, Q. Cui, A. G. Baboul, S. Clifford, J. Cioslowski, B. B. Stefanov, G. Liu, A. Liashenko, P. Piskorz, I. Komaromi, R. L. Martin, D. J. Fox, T. Keith, M. A. Al-Laham, C. Y. Peng, A. Nanayakkara, M. Challacombe, P. M. W. Gill, B. Johnson, W. Chen, M. W. Wong, C. Gonzalez, J. A. Pople, *Gaussian 03*, revision C.02; Gaussian, Inc.: Wallingford, CT, 2004.